

Distributed quantum circuit partitioning and teleportation optimization based on a multi-dimensional evaluation strategy

Le Zhang(张乐), Zhijin Guan(管致锦), Shuo Qin(秦硕), Zheng Luo(罗政), Fei Ding(丁飞), and Xueyun Cheng(程学云)

Citation: Chin. Phys. B, 2026, 35 (**5**): 050305. DOI: 10.1088/1674-1056/ae1c30
http://cpb.iphy.ac.cn; http://iopscience.iop.org/cpb

What follows is a list of articles you may be interested in

Measurement-device-independent quantum key distribution with entanglement-assisted linear Bell state measurement

Cheng Zhang(张诚), Cheng Liu(刘成), Jiawei Ying(应佳伟), Shipu Gu(顾世浦), Lan Zhou(周澜), Yin Ma(马寅), Kang Gao(高亢), Hai Wei(魏海), Kai Wen(文凯), and Yubo Sheng(盛宇波)
Chin. Phys. B, 2026, 35 (**4**): 040310. DOI: 10.1088/1674-1056/ae3605

Hierarchical QAOA circuit design framework for distributed quantum computing

Ting-Yu Luo(骆挺宇) and Yu-Xin Deng(邓玉欣)
Chin. Phys. B, 2026, 35 (**4**): 040309. DOI: 10.1088/1674-1056/ae00ae

Distributed Kuperberg's algorithm

Peng-Yu Yang(杨鹏宇), Xin Zhang(张新), and Song Lin(林崧)
Chin. Phys. B, 2026, 35 (**3**): 030303. DOI: 10.1088/1674-1056/adfb58

Distributed quantum circuit partitioning and optimization based on combined spectral clustering and search tree strategies

Zilu Chen(陈子禄), Zhijin Guan(管致锦), Shuxian Zhao(赵书娴), and Xueyun Cheng(程学云)
Chin. Phys. B, 2025, 34 (**5**): 050305. DOI: 10.1088/1674-1056/adbada

Automatic architecture design for distributed quantum computing

Ting-Yu Luo(骆挺宇), Yu-Zhen Zheng(郑宇真), Xiang Fu(付祥), and Yu-Xin Deng(邓玉欣)
Chin. Phys. B, 2024, 33 (**12**): 120302. DOI: 10.1088/1674-1056/ad7c2c

---

Distributed quantum circuit partitioning and teleportation optimization based on a multi-dimensional evaluation strategy

Le Zhang(张乐)[1], Zhijin Guan(管致锦)[2,1,†], Shuo Qin(秦硕)[1], Zheng Luo(罗政)[1], Fei Ding(丁飞)[1], and Xueyun Cheng(程学云)[1,‡]

[1] *School of Artificial Intelligence and Computer Science, Nantong University, Nantong* 226019, *China*
[2] *College of Engineering the Internet of Things, Taihu University, Wuxi* 214063, *China*

(Received 7 September 2025; revised manuscript received 20 October 2025; accepted manuscript online 6 November 2025)

Distributed quantum computing has emerged as a key approach to extending current quantum computing capabilities, with its performance largely determined by the cost of qubit transmissions across physical nodes. To minimize such cross-partition transmission costs, this paper proposes a distributed quantum circuit partitioning and teleportation optimization method based on a multidimensional evaluation strategy. First, a scoring function is designed using interaction strength and temporal fragmentation, guiding the partitioning process to balance structural compactness with temporal continuity. Building on this, we employ multiple starting points and parameter search strategies to progressively construct candidate partition schemes. Subsequently, a transmission-cost optimization method based on teleportation group partitioning is introduced to evaluate candidates more accurately, taking into account gate timing, interfering operations, and communication resource conflicts, thereby yielding a more realistic estimate of teleportation counts. Simulation results on several benchmark quantum circuits demonstrate that the proposed method consistently generates superior partitions under challenging conditions, such as high interaction density and significant gate interleaving. In some cases, teleportation counts are reduced by up to 64.7%, with an overall average improvement of 8%, verifying the adaptability and effectiveness of the method in optimizing communication across different interaction structures.

Keywords: distributed quantum computing, structure-aware scoring, merged teleportation, qubit partitioning

PACS: 03.67.–a, 03.67.Ac, 03.67.Hk, 03.67.Lx

DOI: 10.1088/1674-1056/ae1c30 **CSTR:** 32038.14.CPB.ae1c30

1. Introduction

In recent years, mainstream platforms such as superconducting circuits and ion traps[1–3] have driven the continuous expansion of qubit counts on quantum chips. Companies like IBM and Google have already demonstrated medium-scale quantum processors of considerable size.[4,5] However, quantum computing is still in the era of noisy intermediate-scale quantum (NISQ),[6] where fundamental bottlenecks such as qubit fidelity, decoherence time, and physical topology constraints pose long-term challenges to the scalability of single-chip systems, thereby motivating research into scalable quantum computing schemes, particularly those based on distributed architectures.

Distributed quantum computing architectures map logical quantum circuits onto multiple physically separated quantum processing units (QPUs) and utilize quantum communication technologies to transmit quantum states across nodes.[7] Such architectures not only enhance system scalability but also provide the foundation for realizing large-scale quantum computing. In this framework, local quantum gates can be executed independently within each QPU, whereas two-qubit gates involving different partitions (i.e., global gates) must be implemented through communication mechanisms such as quantum teleportation.[8] Since these processes rely on pre-shared entanglement, classical information exchange, and inter-chip coordination, their execution cost is significantly higher than that of local gates, making communication a critical bottleneck to overall computational performance.

In distributed quantum systems, optimizing the transmission overhead induced by global gates is crucial not only for system efficiency but also for the effectiveness of key modules such as circuit partitioning and scheduling. Reference [9] introduced the idea of transmission merging, where multiple temporally adjacent global gates are grouped into a single transmission unit to reduce the total number of teleportations. Nonetheless, existing approaches often simplify the execution of this strategy, overlooking qubit resource conflicts during teleportation, the additional cost of return transmissions introduced by certain merges, and temporal dependency constraints among gate operations. These factors are particularly critical in circuits with high structural density; neglecting them may cause significant discrepancies between estimated and actual communication costs, thereby compromising the validity of subsequent partitioning and scheduling.

Extensive research has been devoted to addressing the

†Corresponding author. E-mail: guan.zj@ntu.edu.cn
‡Corresponding author. E-mail: chen.xy@ntu.edu.cn

© 2026 Chinese Physical Society and IOP Publishing Ltd. All rights, including for text and data mining, AI training, and similar technologies, are reserved.

communication cost in quantum circuits by exploring structural optimization of partitioning strategies. For instance, Andres-Martinez *et al.*[10] formulated the distributed mapping problem of quantum circuits as a hypergraph partitioning task and solved it using the KaHyPar partitioning optimizer; Dadkhah *et al.*[11] transformed the quantum circuit into a bipartite graph model and applied a dynamic programming algorithm for partitioning; Reference [12] proposed an efficient partitioning method that integrates gate teleportation and qubit teleportation; Reference [13] employed an integer programming model to minimize the number of global gates, followed by a recursive algorithm to optimize teleportation count; and Ref. [14] introduced an exhaustive approach that enumerates different configurations of global gate execution positions, evaluates the teleportation overhead under each configuration, and selects the scheme with the minimal communication cost to achieve automatic optimization of distributed quantum circuits.

In Ref. [15], Daei *et al.* proposed a method for generating distributed quantum circuits from entire quantum circuits, where communication overhead between components is reduced by optimizing the partitioning strategy. Reference [16] proposes a quantum network scheme based on deterministic quantum gate transmission and modular architecture. By constructing a system composed of superconducting qubit nodes and low-loss communication links, the scheme enables the generation and cross-node distribution of multi-qubit entangled states, with the aim of improving entanglement fidelity in quantum networks and providing a scalable architecture for large-scale quantum computing. Reference [17] presented a partitioning method based on the quadratic unconstrained binary optimization (QUBO) model, enhanced with a dynamic look-ahead strategy to minimize transmission cost. By transforming the partitioning task into a graph min-cut problem and leveraging quantum annealing for accelerated solving, this approach achieved significant reductions in both transmission cost and runtime on benchmark circuits. Reference [18] proposed a genetic algorithm-based optimization of global gate transmission directions, where the direction quality is evaluated to identify the optimal scheme. This method minimizes state transmission costs in distributed quantum circuits, thereby enabling efficient conversion of global gates into local gates and more effective circuit mapping.

Most existing approaches focus on minimizing the number of global gates, relying primarily on structural partitioning strategies of qubit interaction graphs. However, such methods struggle to capture the execution order of quantum gates and scheduling constraints. In circuits with dense operations or strong cross-partition dependencies, reducing the number of global gates does not necessarily lead to fewer teleportations; in some cases, communication pressure may even increase due to failed merging or resource conflicts.

To address this issue, this paper first proposes a qubit partitioning method guided by a partition-adaptability scoring function, which simultaneously considers the interaction strength between qubits and the temporal fragmentation of operations at the scheduling level. This scoring guides the progressive expansion of partitions to balance structural compactness with temporal continuity, thereby producing more adaptive initial partitioning schemes. Subsequently, we introduce a transmission-cost optimization method based on merged teleportation, which incorporates strategies for constructing teleportation groups, detecting scheduling conflicts, and analyzing the overhead of return operations. By leveraging the temporal dependencies of quantum gates and qubit usage patterns, this method enables more fine-grained estimation of teleportations induced by cross-partition operations. Together, these two components not only enhance the rationality of partition construction but also provide a more reliable analytical foundation for communication optimization in distributed quantum circuits.

2. Background

2.1. Distributed quantum computing

Distributed quantum computing (DQC) is a computational architecture in which multiple independent physical QPUs collaboratively perform quantum tasks. In this architecture, each QPU possesses its own qubits and local gate control capabilities, while multiple QPUs are interconnected via quantum communication channels to form a logically unified large-scale quantum system. Currently, mainstream QPU interconnection approaches include static topologies (e.g., linear chains and two-dimensional grids) as well as dynamically reconfigurable mechanisms based on superconducting microwave circuits or optical links.[19] The core function of these communication channels is to enable quantum state transfer across QPUs, which primarily relies on quantum entanglement and quantum teleportation.[20] Specifically, when a two-qubit gate involving qubits located on different QPUs is required, the system first distributes and pre-stores entangled pairs between the two QPUs. By transmitting measurement outcomes over classical channels, the state of one qubit can be temporarily migrated to the other QPU, where the operation is performed, before returning its state afterward.[21]

2.2. Local and global gates

In distributed quantum computing, quantum gates can be categorized into two types based on the locations of their operand qubits: local gates and global gates. If the two operands of a two-qubit gate reside within the same QPU, the gate can be executed locally and is referred to as a local gate. In contrast, if the operands are distributed across

different QPUs, the gate must be executed through coordination over quantum communication links and is referred to as a global gate. Figure 1 illustrates the logical structure of a 6-qubit distributed quantum circuit, where G_3 is a local gate, while G_1, G_2, G_4, and G_5 are global gates. Compared with local gates, the execution of global gates incurs significantly higher costs. In practical quantum circuits, global gates are often the primary source of communication bottlenecks. Accurate estimation of the number of teleportations required for global gates, as well as exploiting their structural mergeability, is crucial for optimizing qubit partitioning and thereby improving the overall communication efficiency of the system.

2.3. Quantum teleportation

According to the no-cloning theorem,[22] it is impossible to obtain the full coefficient information of a qubit in a superposition state through measurement, since once a measurement is performed, the quantum state collapses irreversibly and the original quantum information is lost. Consequently, in quantum communication, a qubit state cannot be directly "copied" to another location via classical channels. Quantum teleportation provides a feasible solution. Its core idea is to transmit a quantum state to a remote location without physically moving the qubit, by leveraging shared entanglement together with classical communication. In this process, the sender and receiver must first establish an entangled qubit pair. The sender then performs a joint measurement (e.g., a Bell-state measurement) on the qubit to be transmitted and the local entangled qubit, and communicates the measurement outcomes to the receiver through a classical channel. Based on this information, the receiver applies the corresponding recovery operations and thereby reconstructs the original quantum state locally.[23]

2.4. Merged teleportation

To reduce communication overhead, Ref. [9] proposed the strategy of merged teleportation, in which multiple global gates that act on the same communication qubit, are temporally adjacent, and free from scheduling conflicts are executed through a single teleportation operation. This approach effectively compresses the total number of teleportations and thereby improves overall communication efficiency. For example, as shown in Fig. 1, global gates G_1 and G_2 are consecutive and share qubit q_3, which allows them to be merged into a single teleportation, reducing the teleportation count from 4 (if executed separately) to 2.

However, in large-scale quantum circuits, the interplay among gate scheduling relations, qubit usage periods, and shared scheduling resources makes the decision of "whether gates can be merged" nontrivial. For instance, as shown in Fig. 1, although global gates G_2 and G_4 both act on the same qubit, the presence of an intervening local gate G_3 breaks their mergeability. Similarly, when multiple teleportation groups share a communication channel, temporal overlaps may result in scheduling conflicts. Therefore, the determination of mergeability must take into account temporal order, interfering gate placement, and communication resource availability in an integrated manner, rather than relying solely on local adjacency analysis.

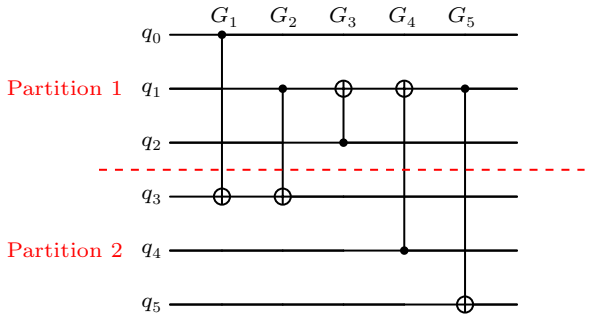


Fig. 1. Example of distributed quantum circuit.

2.5. Motivation

Against this background, the construction of efficient distributed quantum circuits faces two interrelated challenges. On the one hand, the qubit partitioning scheme directly determines the distribution of global gates and the corresponding communication paths; thus, rational partition planning is essential for reducing communication conflicts and teleportation overhead. On the other hand, optimizing the transmission cost induced by cross-partition operations is equally critical for guiding partitioning and scheduling strategies. These two aspects are complementary and together form the foundation of communication optimization in distributed quantum circuits.

3. Quantum circuit partitioning and optimization

In distributed quantum computing, reducing communication overhead relies on constructing low-cost qubit partitioning schemes and optimizing the number of teleportations induced by cross-partition operations. Existing approaches often minimize the number of global gates through methods such as interaction-graph min-cut; however, this metric is not equivalent to the actual teleportation count — multiple temporally adjacent global gates acting on the same teleportation qubit can be merged into a single continuous transmission, thereby significantly reducing the number of teleportations. Relying solely on the global gate count may thus overlook such optimization opportunities. To address this, we incorporate both qubit interaction strength and gate temporal relations, and propose a score-guided partitioning method oriented toward minimizing teleportation cost, which incrementally constructs

qubit groups with strong internal interactions and low transmission overhead.

3.1. Design of partition adaptability scoring function

3.1.1. Interaction intensity and its characterization

In scenarios where a quantum circuit is deployed across multiple physical processing units, if a two-qubit gate acts on two qubits that reside in different partitions, the execution of this gate requires a qubit migration operation.

Definition 1 For a two-qubit gate acting on qubits distributed across different partitions, the gate operation must be completed through a teleportation process involving qubit migration. In this process, the qubit that is actually transmitted across partitions is referred to as the teleported qubit, while the other qubit, which remains in its original physical partition, is called the non-teleported qubit.

To reduce the teleportation cost incurred by cross-partition operations, it is necessary during partition construction to prioritize the selection of qubits that are closely associated with the current partition, thereby converting as many potential global gates as possible into local gates. To this end, we introduce interaction intensity as an indicator in the scoring function, which measures the degree of interaction between a candidate qubit and the qubits already within the current partition.

Specifically, the interaction intensity is defined as the ratio between the number of two-qubit gates jointly involving the candidate qubit q and all qubits in the current partition P, and the total number of gate operations acting on the candidate qubit q. The formula is given

$$\mathrm{IS}(q,P) = \frac{\sum_{q' \in P} \mathrm{Num}(q,q')}{\mathrm{Sum}(q)}. \tag{1}$$

$\mathrm{IS}(q,P)$ denotes the interaction intensity of a candidate qubit q joining the current partition P; q' represents a qubit within partition P; $\mathrm{Num}(q,q')$ denotes the number of gates between the candidate qubit q and qubit q' in the current partition P; and $\mathrm{Sum}(q)$ represents the total number of gate operations on the candidate qubit. A larger ratio indicates that most operations of the candidate qubit are concentrated within the current partition, implying a higher partition adaptability.

For example, as shown in Fig. 1, suppose the qubits in the current partition are q_3, q_4, q_5, and the candidate qubit is q_1. Since the total number of gates between q_1 and the qubits in the current partition is 3, and the total number of gate operations on q_1 is 4, the interaction intensity of q_1 with the current partition is 0.75, indicating that most of its operations involve qubits within the partition and it exhibits good structural compatibility. Therefore, a higher interaction intensity suggests that the qubit is structurally more suited to the current partition.

Definition 2 If multiple global gates consecutively act on the same teleported qubit in the gate sequence of a quantum circuit, and no other gates affecting this qubit appear in between, the resulting subsequence is referred to as a teleportation group.

Within a teleportation group, the teleportation operation can be completed through a single merged teleportation. For example, as shown in Fig. 1, gates G_4 and G_5 satisfy the conditions of Definition 2 and can be treated as a teleportation group with q_1 as the teleported qubit, allowing their operations to be executed via a single merged teleportation.

3.1.2. Temporal fragmentation and its characterization

Interaction intensity reflects the structural closeness of a candidate qubit's interactions, but in actual partitioning, the temporal distribution of operations also affects the overhead of cross-partition teleportation.

Definition 3 If a local gate acts on a teleported qubit and is positioned between two global gates in the gate sequence, thereby preventing them from being merged into the same teleportation group, the gate is referred to as an interfering gate.

When interaction operations are too dispersed, communication overhead tends to increase. To address this, we further introduce a metric called temporal fragmentation, which quantifies the degree of temporal dispersion through gate sequence analysis. By assigning each qubit a unique binary code and recording the temporal positions of gate operations in the circuit, we construct a sequence of qubit codes arranged according to operation order. The number of changes in qubit codes within this sequence is then used as an estimate of temporal fragmentation.

For better illustration, we visualize this metric using colored coding corresponding to the binary identifiers, showing the fragmentation of a subsequence of gates. Each qubit is assigned a distinct color, and the color sequence is drawn according to the gate order in the circuit.

The more frequent the color switches, the more often the operations of the candidate qubit are interleaved with those of qubits in the original partition, making it more difficult to merge them into a single teleportation group. This may ultimately result in the splitting of teleportation counts and an increase in transmission cost. The formula is given

$$\mathrm{SP}(q) = \frac{\mathrm{Num}_{\mathrm{switch}}}{\mathrm{Num}_{\mathrm{total}}}. \tag{2}$$

$\mathrm{Num}_{\mathrm{switch}}$ denotes the number of times the qubit identifier changes, and $\mathrm{Num}_{\mathrm{total}}$ represents the length of the time-ordered sequence formed by all gate operations after adding the candidate qubit q to the original partition. A higher ratio indicates that the operations of the candidate qubit are more frequently interleaved within the gate sequence of the current partition, which can disrupt the formation of teleportation

groups among the qubits already in the partition, thereby increasing the transmission cost.

For example, as shown in Fig. 2, the color sequence changes as red → yellow → green → red → green → yellow, counting 5 switches. The fragmentation metric SP is then calculated as $5/8 = 0.625$, where 8 is the length of the subsequence.



Fig. 2. Schematic of temporal coloring.

This ratio quantifies the frequency of qubit identifier changes in gate operations and reflects the degree to which the candidate qubit's operations interleave with those of the original partition qubits in the temporal execution sequence. A higher switching frequency means the candidate qubit's gates are more frequently interspersed among the current partition's gates, potentially introducing interruptions into originally continuous and mergeable teleportation counts, breaking the original scheduling structure. This can split teleportation groups and increase communication overhead. Subsection 3.3.1 further demonstrates, through examples, the correlation between this metric and teleportation cost, highlighting its key guiding role in partitioning strategies.

3.1.3. Partition fitness scoring function

To reflect the optimization objective of encouraging communication intensity while suppressing temporal fragmentation from a global structural perspective, the following scoring function is designed as

$$\text{score}(q) = \frac{{b_1}^{\text{IS}(q,P)}}{{b_2}^{\text{SP}(q)}}. \tag{3}$$

This function assigns a composite score to the candidate qubit q, where b_1 and b_2 serve as the bases of the exponential terms, adjusting the weighting of interaction strength and temporal fragmentation in the final score, respectively. A higher score indicates that the candidate qubit has a stronger compatibility with the current partition. We use an exponential form to capture the nonlinear, threshold-like effect of interaction intensity and temporal fragmentation on partition adaptability.

As shown in Eq. (3), the positive exponential term $b_1^{\text{IS}(q,P)}$ reflects that higher interaction strength leads to a higher score, while the negative exponential term $b_2^{\text{SP}(q)}$ reflects that greater temporal fragmentation results in a lower score.

A higher interaction strength indicates that the candidate qubit shares more gate connections with the current partition. If it is assigned to this partition, more originally cross-partition global gates can be transformed into local gates, thereby effectively reducing transmission costs.

Suppose the candidate qubit q has n two-qubit gates with qubits in the current partition. In this case, its maximum communication benefit corresponds to saving $2n$ teleportation counts (including forward migration and state return). However, not all gates can necessarily be merged into local gates; some may still require teleportation due to temporal interleaving, path conflicts, or other constraints. In the worst-case scenario, even if merging fails, these gates can at least be executed along a single continuous path, yielding a theoretical lower bound of saving 2 teleportations.

Thus, the range of teleportation compression enabled by interaction strength is defined as

$$2 \le T_{\text{saved}} \le 2n. \tag{4}$$

This result indicates that interaction strength essentially reflects the communication integration potential of a candidate qubit. The higher its value, the greater the merging space between the candidate qubit and the current partition, enabling more effective transformation of global gates into local gates and thereby compressing the total number of communications.

Table 1, using the circuit in Fig. 3 as an example, illustrates the interaction among different qubits, where the initial qubit of the current partition is set as q_0. In the qubit selection process, the qubit q_4, which interacts most with q_0, is chosen. There are two two-qubit gates between q_0 and q_4, and q_4 is involved in a total of four gate operations, resulting in an interaction strength of 0.5. After adding q_4 to the current partition, the two global gates at positions 3 and 4 in the gate sequence can be directly converted into local gates, saving up to four teleportations and thereby reducing the communication cost.

Table 1. Interaction table.

Qubit	Gate operations	Interaction count with other qubits					
		q_0	q_1	q_2	q_3	q_4	q_5
q_0	1, 3, 4, 5, 6	0	1	0	1	2	1
q_1	2, 5, 7, 8	1	0	1	1	0	1
q_2	8	0	1	0	0	0	0
q_3	1, 2	1	1	0	0	0	0
q_4	3, 4	2	0	0	0	0	0
q_5	6, 7	1	1	0	0	0	0

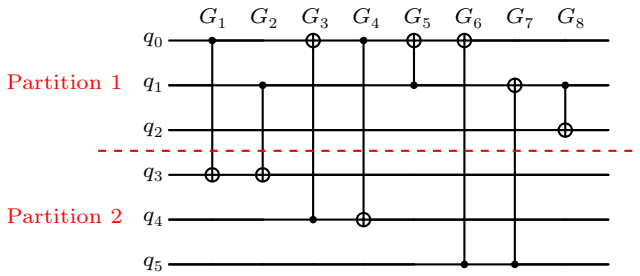


Fig. 3. Example of a 6-qubit circuit.

Temporal fragmentation measures the extent to which the operations of a candidate qubit are interleaved with those of other qubits in the current partition within the gate sequence.

Essentially, it reflects the degree of disruption to the coherence of existing teleportation groups. A higher fragmentation value indicates that the candidate qubit's operations more frequently interrupt the teleportation groups formed by qubits in the current partition, causing potential merged teleportation groups to be split into multiple subsections, and thereby increasing the number of teleportations.

To characterize its impact, assume that a teleportation qubit in the original partition has m consecutive global gate operations, which, in the absence of interference, can be merged into a single group requiring only one teleportation (or at most two, including the return). If the addition of a candidate qubit q breaks this group into k segments, the teleportation group is forced to split into k subgroups, and the teleportation count may increase to at most $2k$. In this case, the extra communication overhead introduced by q is bounded above by $2(k-1)$ and below by 0 (i.e., when q does not interfere with any teleportation group). Therefore, the transmission cost is given

$$0 \leq T_{\text{added}} \leq 2(k-1). \tag{5}$$

In summary, the interaction strength represents the potential benefit of a candidate qubit in reducing the number of teleportations, while the temporal fragmentation reflects the additional overhead that may be introduced when the candidate qubit is incorporated into a partition. Combining the two in the form of a numerator and denominator intuitively captures the basic principle that "the greater the benefit, the higher the score; the greater the cost, the lower the score."

3.2. Partition construction

The scoring function is not only used to evaluate the interaction strength and temporal fragmentation of candidate qubits, but also directly guides the partition construction process. In the proposed method, each partition begins with a single qubit, and under the guidance of the scoring function, the highest-scoring candidate qubits are gradually merged until the size and balance constraints are satisfied.

Definition 4 If a qubit is the first to be assigned to a partition during the construction process, it is defined as the starting qubit.

Table 2. Partition construction steps with q_0 as the starting point

Step	Expanded partition	Timeline	Interaction strength	Temporal fragmentation	Score
I	q_0+q_4	1 3 4 5 6	1	0.4	3.79
	q_0+q_1	1 2 3 4 5 6 7 8	0.25	0.25	1.26
	q_0+q_3	1 2 3 4 5 6	0.5	0.17	1.99
	q_0+q_5	1 3 4 5 6 7	0.5	0.33	1.78
II	$q_0+q_4+q_1$	1 2 3 4 5 6 7 8	0.25	0.5	1.06
	$q_0+q_4+q_3$	1 2 3 4 5 6	0.5	0.5	1.58
	$q_0+q_4+q_5$	1 3 4 5 6 7	0.5	0.67	1.41

Table 3. Partition construction steps with q_1 as the starting point.

Step	Expanded partition	Timeline	Interaction strength	Temporal fragmentation	Score
I	q_1+q_0	1 2 3 4 5 6 7 8	0.25	0.625	0.97
	q_1+q_2	2 5 7 8	1	0.25	4.20
	q_1+q_3	1 2 5 7 8	0.5	0.4	1.69
	q_1+q_5	2 5 6 7 8	0.5	0.6	1.48
II	$q_1+q_2+q_0$	1 2 3 4 5 6 7 8	0.2	0.75	0.82
	$q_1+q_2+q_3$	1 2 5 7 8	0.5	0.6	1.48
	$q_1+q_2+q_5$	2 5 6 7 8	0.5	0.4	1.69

Since the expansion process originates from the starting qubit, all subsequent candidate sets and score calculations are influenced by it. Therefore, different starting qubits may lead to entirely different partitioning results. If the partition construction begins from only one starting qubit, the solution may become trapped in a local optimum determined by the local structure around that qubit. To address this issue, this work introduces a multi-start strategy: first, several qubits with the highest number of gate occurrences are selected as candidate starting points; then, partitions are constructed separately from each of these starting qubits; finally, among these candidate partitions, the one with the minimum number of teleportations is selected to improve the robustness of the overall scheme. Tables 2 and 3 illustrate the partitioning variations arising from different starting qubits.

Table 2 presents the step-by-step expansion process for the circuit in Fig. 3 when q_0 is chosen as the starting qubit. The parameters of the scoring function are set to $b_1 = 5$ and $b_2 = 2$ as an illustrative example to demonstrate the calculation procedure and the partition expansion trend. Different colors represent potential merged teleportation groups formed around the same teleportation qubit. All local gates are marked in yel-

low. First, for the candidate qubits $\{q_1, q_3, q_4, q_5\}$, the scores are computed according to Eq. (3). Among them, the combination $q_0 + q_4$ achieves the highest score with an interaction strength of 1 and a temporal fragmentation of 0.40, corresponding to a score of 3.79. Thus, q_4 is merged with q_0, yielding the current partition $[q_0, q_4]$. Next, for the updated partition, the candidates $\{q_1, q_3, q_5\}$ are evaluated: q_3 is selected, resulting in the partition $[q_0, q_4, q_3]$. Under the target size constraint, this round of expansion terminates, and the final partition is $[q_0, q_4, q_3]$, while the remaining qubits are assigned to the other partition.

3.3. Transmission cost optimization

After the partitioning is completed, the next step is to evaluate the resulting communication overhead. For distributed quantum circuits, the number of teleportations serves as a key metric for assessing the quality of a partitioning scheme. If each cross-partition two-qubit gate is simply counted as one forward transmission and one return, the resulting estimate is often overly inflated. Although some existing methods attempt to merge adjacent gates into a single transmission, they still cannot fully address scheduling constraints and continuous teleportation merging.

Taking Fig. 3 as an example, the global gates G_3 and G_4 are temporally adjacent and act on the same teleportation qubit, allowing them to be executed with a single transmission for both operations, thereby reducing the teleportation count from four to two. Furthermore, if the qubit is not used afterward, the return step can be omitted, leaving only one transmission in total. The proposed method addresses this by grouping consecutively schedulable global gates into the same teleportation group, enabling multiple global gates to be executed with a single teleportation, thereby significantly reducing the overall teleportation count.

3.3.1. Evaluation of candidate teleportation qubits

In the proposed method, when processing each global gate, it is necessary to select one of the two qubits belonging to different partitions as the teleportation qubit. The method then attempts to identify a structurally continuous group of global gates centered on this qubit — that is, multiple global gates that act consecutively on the same qubit without being interrupted by interference gates. Such gates can be grouped together and executed within a single teleportation process, thereby reducing redundant transmission costs.

To evaluate which of the two qubits is more advantageous for constructing a teleportation group, this work introduces a scoring function designed to measure their potential for group-wise transmission consolidation as well as the associated transmission cost. Accordingly, the scoring function can be expressed as

$$\mathrm{Score}(i) = \alpha M^* - \beta R_i. \tag{6}$$

Here, M^* denotes the sum of the scores of the subsequent global gates acting on a given qubit, while R_i indicates whether the teleportation group requires the quantum state to be sent back, represented by 1 or 0. The calculation formula for M is given

$$M^* = \sum_{x=1}^{m} M_x, \tag{7}$$

$$M_x = \frac{1}{2^d}, \quad d \in \{0,1,2,\ldots,n\}, \quad x \in \{1,2,3,\ldots,m\}. \tag{8}$$

Here, α and β denote coefficients, M_x denotes the individual score of the x-th global gate on the qubit, and d represents the number of interfering gates between this gate and the current teleportation group. In the scoring function, a weighting factor of 2^{-d} is applied to each candidate gate in the form of exponential decay, reflecting the difficulty of being incorporated into the teleportation group. Ultimately, the qubit with the higher score is selected as the teleportation qubit.

The design of this function is based on structural analysis of multiple quantum circuits. When the number of interfering gates between the target gate and the teleportation group is small, the feasibility of incorporating it into the teleportation group through gate commutation rules is significantly improved. However, as the number of intermediate gates increases, the success rate of such structural adjustments decreases rapidly.

To validate the rationality of the above scoring function, the following experimental procedure was designed:

Step 1: Choose a global gate as the target gate.

Step 2: Randomly construct a set of local gates on the control or target qubits of the teleportation group (i.e., interference gates), and insert these gates between the teleportation group and the target global gate to form a complete circuit.

Step 3: Gradually attempt to move the interference gates between the target global gate and the teleportation group according to gate commutation rules, simulating the process of merging the target gate into the current teleportation group.

Step 4: For circuits with a given number of interference gates, repeat the above process multiple times (e.g., 100 trials), and compute the merge success rate as the ratio of the number of trials where all interference gates were successfully removed to the total number of trials.

The simulation results are shown in Fig. 4. As the number of interference gates increases, the merge success rate shows a rapidly decreasing trend, which approximately follows an exponential-like decay pattern. This phenomenon is strongly consistent with the weight design in the scoring function, further confirming that the degree of structural interference is a key factor affecting the feasibility of gate merging.

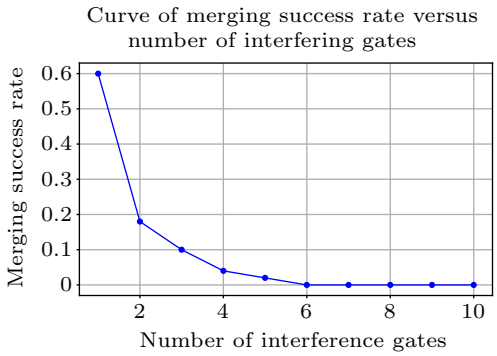


Fig. 4. Line chart of merging success rate versus the number of interference gates.

On the other hand, the R_i term reflects the operational cost of returning the quantum state to its original partition. In some cases, if the qubit is no longer involved in subsequent gate operations after merging, the return operation can be avoided, thereby saving one teleportation.

Through this scoring function, the system can reasonably estimate the "merging potential" of each qubit as a teleportation qubit. After selecting the qubit with the highest score, a new teleportation process is established based on the corresponding gate, and its complete covered time interval is recorded. This helps dynamically identify and construct feasible teleportation optimization paths without changing the qubit partitions, significantly improving the utilization efficiency of communication resources.

As shown in Fig. 3, consider a distributed quantum circuit containing 6 qubits, which is partitioned into two subsets. To compute the inter-partition teleportation count for this circuit, the gate sequence is first scanned according to the partition information to identify two-qubit gates acting on qubits from different partitions, i.e., the global gates. A total of 6 global gates are identified: G_1, G_2, G_3, G_4, G_6, and G_7, while G_5 and G_8 are local gates (both of their qubits reside in the same partition).

After identifying all global gates, the construction of teleportation groups begins. The process starts with the global gate G_1, attempting to form the first teleportation group. G_1 acts on qubits q_0 and q_3, so both are evaluated as candidate teleportation qubits.

If q_0 is selected as the teleportation qubit, then among its subsequent gates, G_3 and G_4 also act on q_0, and there are no interfering gates between them and G_1. Therefore, their individual scores are both 1. Global gate G_6 also acts on q_0, but a local gate G_5 acting on q_0 precedes it, introducing interference. According to the scoring model, the score for G_6 is computed as $2^{-d} = 0.5$.

Qubit q_0 is no longer used after gate G_4. However, gate G_6 still requires this qubit, so a return operation is necessary, resulting in a return cost of $R = 1$. To maintain a balanced influence between the benefits of mergeable operations and the cost of the return process, the parameters are set as $\alpha = 3$ and $\beta = 1$, where α amplifies the contribution of mergeable gates and β corresponds to the one-time return overhead within each teleportation group. Accordingly, the partial scores sum to $3(1 + 1 + 0.5) = 7.5$. After subtracting the return cost, the final total score for using q_0 as the teleportation qubit is $7.5 - 1 = 6.5$.

3.3.2. Teleportation group construction

In the process of constructing a teleportation group, selecting a teleportation qubit is only the initial step. Whether the group can be further expanded to include multiple global gates depends on the arrangement of these gates in the gate sequence and the presence of intervening interference. In theory, if several global gates are relatively adjacent in the logical gate sequence and all act on the same teleportation qubit, they can potentially be executed sequentially through a single teleportation operation, forming an effective teleportation group.

(1) Handling interference gates In practical circuits, interference gates can block the further expansion of a teleportation group. To maximize the size of a teleportation group, we leverage the commutation rules of quantum gates. While preserving the logical equivalence of the circuit, we attempt to adjust the local gate order of the interference gates to determine whether they can be moved out of the time interval of the current candidate gate segment. This clears obstacles to expansion and enables a larger range of gate merging.

For example, Fig. 5 illustrates two typical CNOT gate commutation scenarios: when two CNOT gates share the same control qubit but have different target qubits, their order can be equivalently swapped; similarly, when two gates share the same target qubit but have different control qubits, they can also be exchanged.

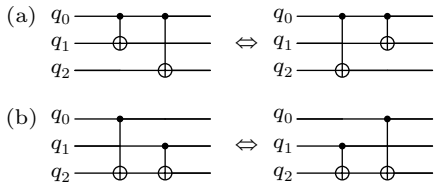


Fig. 5. Equivalent swap circuits shown in panels (a) and (b).

If the interference gates cannot be cleared through commutation, the current teleportation group expansion terminates, and the already merged global gates form a complete teleportation group.

For the example in Fig. 3, after determining the teleportation qubit for teleportation group 1 as q_0, there are no interference gates between G_1, G_3, and G_4, so these gates can be merged.

For gate G_6, there is an interference gate G_5 between it and G_4, so an attempt is made to move G_5 out of the teleportation interval of group 1 using gate commutation rules to avoid interference.

Although gate G_2 does not interfere with teleportation group 1, it is still attempted to be moved out of the teleportation interval to maximize gate merging.

The constructed teleportation group 1 is shown in Fig. 6. The movement of interfering gates after constructing teleportation group 1 is shown in Fig. 7.

Finally, the circuit after moving G_2 and G_5 out of the teleportation interval of group 1 is shown in Fig. 8, with the teleportation interval of group 1 being $(1,4)$.

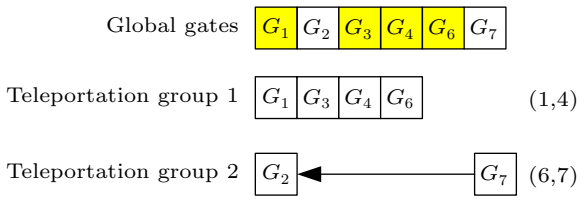


Fig. 6. Illustration of teleportation group construction.

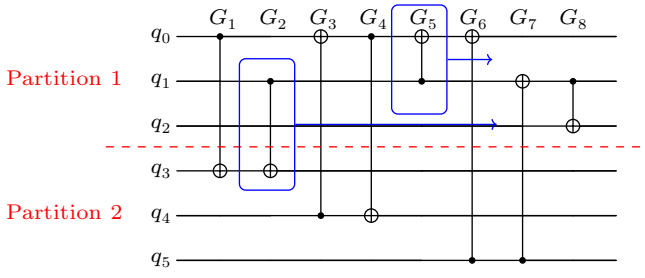


Fig. 7. Movement of interfering gates after constructing teleportation group 1.

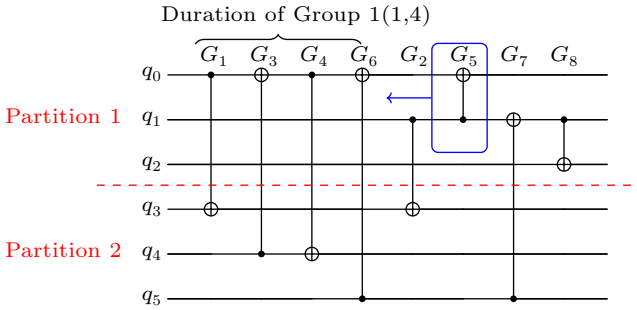


Fig. 8. Movement of interfering gates after constructing teleportation group 2.

Next, teleportation group 2 is constructed. According to the scoring function, the teleportation qubit for group 2 is determined as q_1.

Since there is an interference gate G_5 between G_7 and G_2, G_5 is attempted to be moved out of the teleportation interval.

Figure 9 shows the final circuit after moving G_5 out of the teleportation interval of group 2, with the teleportation interval of group 2 being $(6,7)$.

(2) Handling scheduling conflicts After all teleportation groups have been constructed, their actual executability must still be verified. In the distributed quantum computing model, only one teleportation task can occupy a communication channel at any given time.

If multiple teleportation groups have overlapping time intervals, even if they involve different qubits, they cannot be scheduled simultaneously due to resource conflicts. When the scheduling times of two teleportation groups overlap, the system treats it as a conflict and removes the conflicting group from the current scheduling stage; the associated global gates will be rescheduled in subsequent stages.

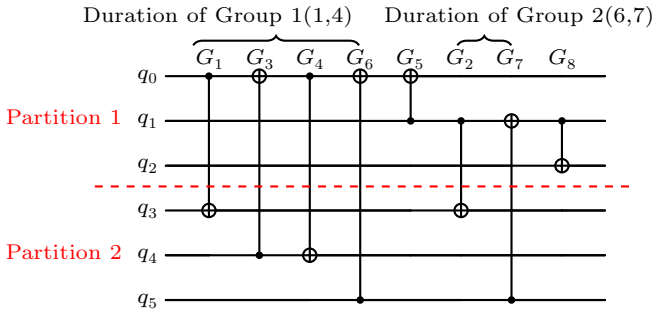


Fig. 9. The final transformed circuit.

Algorithm 1 Transmission cost optimization

Input: Quantum gate sequence G, partitions $P1$, $P2$.
Output: Total number of teleportations T.

$GG \leftarrow$ get_global_gates$(G, P1, P2)$ ▷ Extract cross-partition gates
$Grps \leftarrow \emptyset$ ▷ Initialize teleportation groups
for $g \in GG$ **do**
  merged $\leftarrow$ false
  for $grp \in Grps$ **do**
    if g shares teleportation qubit with grp **and** no_intf$(grp.end, g.idx)$ **and** no_overlap(grp, g) **then**
      merge g into grp
      $grp.end \leftarrow g.idx$
      merged $\leftarrow$ true
      break
  if not merged **then**
    $btq \leftarrow \arg\max_{tq} \left(\alpha \cdot M^*(tq) - \beta \cdot R_i(tq)\right)$
    if $btq \neq$ None **then**
      add new group $\{tq : btq, start : g.idx, end : g.idx\}$ to $Grps$
$T \leftarrow 0$ ▷ Initialize teleportation count
for $grp \in Grps$ **do**
  if tq_used_after$(grp.end)$ **then**
    $T \leftarrow T + 2$ ▷ Teleportation + return
  else
    $T \leftarrow T + 1$ ▷ Single teleportation
return T

For example, in Fig. 9, teleportation group 1 has a teleportation interval of $(1,4)$, and group 2 has an interval of $(6,7)$. Since the intervals do not overlap on the time axis, they can be scheduled in parallel, and no communication conflict occurs.

This scheduling conflict verification strategy ensures the global schedulability of the constructed teleportation groups, significantly distinguishing it from traditional methods that

roughly estimate communication overhead based solely on the number of global gates. By introducing dynamic conflict detection at the scheduling level, the proposed method better fits practical systems with limited resources. The pseudocode of the transmission cost optimization algorithm is given in Algorithm 1.

3.4. Optimal partition selection

3.4.1. Design of parameter search space

To enhance the adaptability of the scoring function across quantum circuits with different structures, this work introduces a discrete search strategy for the two key tuning parameters b_1 and b_2 in the scoring function, constructing a finite parameter space for adaptive optimization. In the scoring function, b_1 controls the exponential amplification of the interaction strength, while b_2 governs the exponential decay of temporal fragmentation. These parameters directly affect the relative priority of candidate qubit scores and thus play a crucial role in guiding the partitioning structure.

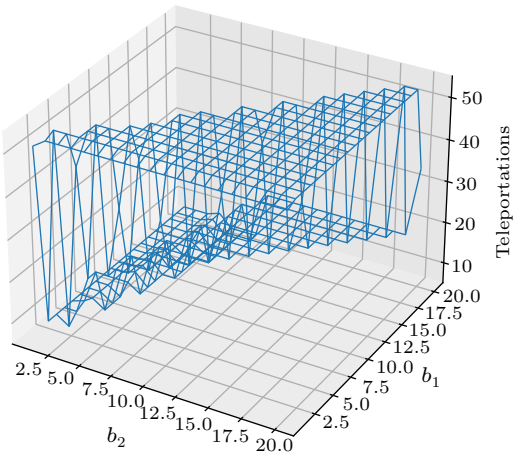


Fig. 10. Effect of different parameters on circuit teleportation count.

To construct an efficient and controllable parameter space, a discrete set of integers is preset (e.g., $\{2,4,6,8,10\}$) as the search range, and all combinations of b_1 and b_2 are traversed. As shown in Fig. 10, different parameter pairs lead to varying teleportation counts for the "cycle10_293" circuit. This circuit originates from the standard reversible circuit benchmark library *RevLib*, and it is commonly used in comparative experiments. Figure 10 illustrates the variation in teleportation counts under different parameter combinations. The overall trend exhibits an upward pattern from the lower-left to the upper-right of the figure, but a distinct plateau appears in the high-value region. This phenomenon is not due to any intrinsic regularity of the algorithm; rather, it arises because a display limit (maximum value of 50) was set for teleportation counts during plotting. The actual teleportation counts for some parameter combinations exceed this threshold, and thus appear truncated as flat regions in the figure.

This design balances the controllability of the parameter space with the expressive capability of the scoring function, avoiding overfitting caused by an excessive number of parameters while retaining effective control over partitioning behavior. In the next section, evaluation and selection will be performed within this parameter space to identify the optimal configuration for constructing the final partitioning scheme.

Algorithm 2 Partition optimization algorithm

Input: Quantum gate sequence G, qubit set $QUBITS$, target partition number $NParts$.
Output: Best partition result $BestRes$ and its evaluation $(b1, b2)$.

$QGMap, IMat \leftarrow$ build_struct(G); // Build qubit interaction map and matrix
$CandSt \leftarrow$ rank_qubits_by_gate(G, K); // Select top-K candidate start qubits
$BestRes \leftarrow null$, $BestTp \leftarrow \infty$, $BestGlb \leftarrow \infty$;
for $sq \in CandSt$ **do**
  $Parts \leftarrow \{\{sq\}\}$; // Initialize first partition
  $Unasg \leftarrow QUBITS \setminus \{sq\}$; // Unassigned qubits
  while $|Parts| < NParts$ **do**
    $sd \leftarrow \arg\max_q \in Unasg$gate_cnt$(q)$; // Pick qubit with most gates
    $NewP \leftarrow \{sd\}$; $Unasg \leftarrow Unasg \setminus \{sd\}$
    while not full($NewP$) **do**
      for $q \in Unasg$ **do**
        $inter \leftarrow \mathrm{IS}(q, NewP)$ // Interaction strength
        $col \leftarrow \mathrm{SP}(q, NewP)$ // Temporal separation
        $Score[q] \leftarrow (b_1^{inter})/(b_2^{col})$;
      $best_q \leftarrow \arg\max_qScore[q]$;
      $NewP \leftarrow NewP \cup \{best_q\}$;
      $Unasg \leftarrow Unasg \setminus \{best_q\}$;
    $Parts \leftarrow Parts \cup \{NewP\}$;
  assign_remain($Unasg, Parts$) // Assign remaining qubits to balance partitions
  opt_gates($G, Parts$) // Optional gate reordering
  $TpCnt \leftarrow$ comp_tp($Parts, G$) // Teleportation count
  $GlbCnt \leftarrow$ cnt_glb_gates($Parts, G$) // Global conflict count
  if $TpCnt < BestTp$ **or** ($TpCnt == BestTp$ **and** $GlbCnt < BestGlb$) **then**
    $BestRes \leftarrow Parts$;
    $BestTp \leftarrow TpCnt$;
    $BestGlb \leftarrow GlbCnt$;
    $BestPar \leftarrow (b1, b2)$;
return $BestRes, BestPar$;

3.4.2. Partitioning optimization algorithm

In this section, the previously proposed scoring function is combined with the transmission cost optimization method to automatically generate and screen partitioning schemes. After setting the parameters, the core objective of the optimization algorithm is to integrate partition construction with trans-

mission cost optimization, thereby identifying the partition scheme with the lowest overall transmission cost. Specifically, the algorithm first selects multiple candidate starting qubits from those with the highest gate counts. Guided by the scoring function, it incrementally constructs partitions until complete partitions satisfying the size constraints are generated. Then, the transmission cost method introduced earlier is applied to evaluate the transmission cost of each partition scheme built from different starting qubits, recording their teleportation counts and the number of global gates. Among all partition schemes, the one with the lowest teleportation count is chosen as the final output. If multiple schemes have the same teleportation count, the number of global gates is used as a secondary criterion to select the better solution. The pseudocode of the partition optimization algorithm is given in Algorithm 2.

4. Results and discussions

The method proposed in this work is implemented using Python. The experimental environment consists of a Ryzen 9 7945HX CPU @ 2.50 GHz with 16 GB of memory. To conduct a representative performance evaluation, we first selected Quantum Fourier Transform (QFT) circuits, which feature a regular structure and rapidly increasing gate counts, and directly compared our method with the strategy proposed in Ref. [18]. That reference employs a heuristic routing and graph partitioning approach aimed at minimizing both the number of teleportation groups and the total number of teleportations, reflecting a typical current methodology for cross-partition operation scheduling optimization.

We conducted experiments on QFT circuits with 4, 8, 16, and 32 qubits, and recorded the total number of teleportations for each circuit, comparing the results with those reported in the literature. Table 4 presents the comparison of teleportation counts under different methods. In Table 4, 'Q' denotes the number of qubits in the circuit, 'G' denotes the number of global gates in the partition, 'TC' represents the teleportation count, and 'Imp' denotes the optimization rate of teleportations, defined as the ratio of the reduction in teleportations relative to the reference method. As shown in Table 4, with the increase in qubit number, the advantage of our method in reducing teleportation becomes more significant. Compared with the method in Ref. [19], our approach reduces the teleportation count by approximately 29.2% and 39.4% on 32-qubit and 64-qubit QFT circuits, respectively. These results indicate that the partitioning scheme guided by our method effectively lowers communication overhead through fewer teleportations.

To comprehensively evaluate the adaptability of our method across different types of circuits, we conducted experiments on several conventional benchmark circuits from RevLib. These circuits feature complex structures, irregular distributions of global gates, higher gate densities, and stronger temporal interleaving, which better reflect the robustness and performance limits of partitioning strategies in practical scenarios. For a thorough evaluation, we compared our method with those in Refs. [17,19], and the simulation results are summarized in Table 5.

Table 4. Comparison results of QFT circuits.

Circuit	Q	G	TC[18]	Ours	Imp
4-qubit QFT	4	4	4	4	0%
8-qubit QFT	8	22	12	10	16.7%
16-qubit QFT	16	82	26	22	15.4%
32-qubit QFT	32	298	65	46	29.2%
64-qubit QFT	64	1114	155	94	39.4%
Average Improvement Rate					20.14%

Table 5. Comparison results of benchmark circuits.

Circuits	Q	G	TC[19]	TC[17]	Ours	IMP
4gt12-v0_87	6	56	29	18	18	0%
4gt4-v0_72	6	47	31	20	20	0%
alu-v2_30	6	119	69	48	46	4.2%
mod5adder_127	6	128	75	47	46	2.1%
sf_274	6	160	129	44	44	0%
hwb5_53	6	324	241	132	128	3%
rd53_138	8	33	11	6	6	0%
cm82a_208	8	86	29	22	21	4.5%
rd53_251	8	253	133	81	83	-2.5%
Ising_model_10	10	10	10	10	10	0%
mini_alu_305	10	28	7	7	5	28.6%
rd73_140	10	59	15	11	7	36.4%
sys6-v0_111	10	36	15	10	9	10%
ham7_299	21	51	38	14	11	21.4%
sym9_317	27	64	69	14	21	-50%
cycle10_293	39	59	79	17	6	64.7%
ham15_298	45	105	55	29	25	13.8%
Average improvement rate						8.01%

Table 5 presents the teleportation count evaluation of our method on multiple conventional quantum circuits, along with a comparison against two baseline approaches. Overall, our method achieves superior performance on most circuits. For circuits such as `mini_alu_305`, `rd73_140`, and `cycle10_293`, the teleportation counts are significantly reduced relative to the baselines, with a maximum reduction of 64.7%. These circuits generally exhibit pronounced temporal interleaving and dense local gates, indicating that our method can effectively guide qubit partitioning to substantially reduce cross-partition operations.

The circuits `sym9_317` and `rd53_251` have highly symmetric and interleaved gate structures, where only a few global gates can be merged continuously. As a result, the merging strategy is less effective, and additional return operations slightly increase the number of teleportations. This is a localized phenomenon inherent to such circuit structures rather than a limitation of the proposed algorithm.

For medium- and large-scale circuits, exemplified by `ham7_299` and `ham15_298`, our method demonstrates stable optimization capability, reducing teleportation counts by 21.4% and 13.8%, respectively. This further validates the adaptability and scalability of our partitioning approach. Meanwhile, for circuits such as `mod5adder_127`, `sf_274`, and `Ising_model_10`, all three methods yield identical teleportation counts, indicating that for circuits with regular structures and well-defined partition boundaries, the choice of partitioning strategy has minimal impact on communication overhead.

Overall, the simulation results demonstrate that the proposed partition scoring strategy consistently achieves favorable transmission cost performance across diverse quantum circuits. Notably, it offers significant advantages in circuits with complex structures and dense operations, highlighting its potential for practical applications.

5. Conclusion

This work addresses the qubit partitioning problem in distributed quantum computing and proposes a partition-adapted distributed qubit partitioning and teleportation cost optimization method. The approach includes two key innovations:

First, a scoring function combining interaction strength and temporal span is designed to guide the partitioning process, balancing structural compactness and temporal continuity. By integrating a multi-start strategy and parameter search, this enables more stable and better-adapted partition construction for large-scale quantum circuits.

Second, a teleportation group-based cost optimization method is introduced, which accurately estimates the required teleportations by considering gate temporal order, the arrangement of interfering gates, and communication resource conflicts.

Simulation results on several representative quantum circuits demonstrate that, compared with existing teleportation cost estimation strategies, the proposed method achieves lower teleportation counts on both QFT circuits and conventional logic circuits.

Acknowledgments

Project supported by the National Natural Science Foundation of China (Grant No. 62072259), in part by the Natural Science Foundation of Jiangsu Province (Grant No. BK20221411), in part by the Natural Science Foundation of Nantong (Grant No. JC2024100), and in part by the Ph.D. Start-up Fund of Nantong University (Grant No. 23B03).

References

[1] Memon Q A, Al Ahmad M and Pecht M 2024 *Quantum Rep.* **6**, 627
[2] Stassi R, Cirio M and Nori F 2020 *npj Quantum Information* **6**, 67
[3] Hamilton M C, Yelamanchili B, Shah A, Peek S E, Bankson S and Tillman C C 2022 *Superconducting Microwave Interconnect Technologies for Quantum and Cryogenic Systems*, IEEE/MTT-S International Microwave Symposium (IMS), 72
[4] Polikarpov P V, Uvarov N K and Khomonenko A D 2021 *Intell. Transp. Syst. Transp. Security* **1**, 33
[5] AbuGhanem M 2024 *arXiv:2410.00916 [quant-ph]*
[6] Preskill J 2018 *Quantum* **2**, 79
[7] Monroe C, Raussendorf R, Ruthven A, Brown K R, Maunz P, Duan L M and Kim J 2014 *Phys. Rev. A* **89**, 022317
[8] Chou K S, Blumoff J Z, Wang C S, Reinhold P C, Axline C J, Gao Y Y and Schoelkopf R J 2018 *Nature* **561**, 368
[9] Ghodsollahee I, Davarzani Z, Zomorodi M, Pawiak P, Houshmand M and Houshmand M 2021 *Quantum Inf. Process.* **20**, 235
[10] Andres-Martinez P and Heunen C 2019 *Phys. Rev. A* **100**, 032308
[11] Dadkhah D, Zomorodi M and Hosseini S E 2022 *IEEE Access* **10**, 70329
[12] Nikahd E, Mohammadzadeh N, Sedighi M and Zamani M S 2021 *Phys. Scr.* **96**, 035102
[13] Davarzani Z, Zomorodi M and Houshmand M 2022 *Sci. Rep.* **12**, 15421
[14] Zomorodi-Moghadam M, Houshmand M and Houshmand M 2018 *Int. J. Theor. Phys.* **57**, 848
[15] Daei O, Navi K and Zomorodi-Moghadam M 2020 *Int. J. Theor. Phys.* **59**, 3804
[16] Zhong Y, Chang H S, Bienfait A, Dumur E, Chou M H, Conner C R, Grebel J, Povey R G, Yan H, Schuster D I and Cleland A N 2021 *Nature* **590**, 571
[17] Chen X, Chen Z, Zhu P, Cheng X and Guan Z 2025 *IEEE Trans. Comput.-Aided Des. Integr. Circuits Syst.*
[18] Chen Z, Chen X, Jiang Y, Cheng X and Guan Z 2023 *Int. J. Theor. Phys.* **62**, 255
[19] Daei O, Navi K and Zomorodi M 2018 *Int. J. Theor. Phys.* **60**, 3494
[20] Pirandola S, Eisert J, Weedbrook C, Furusawa A and Braunstein S L 2015 *Nature Photonics* **9**, 641
[21] Brown K R, Kim J and Monroe C 2016 *npj Quantum Information* **2**, 1
[22] Jozsa R 2004 *IBM J. Res. Dev.* **48**, 79
[23] Verma V and Prakash H 2016 *Int. J. Theor. Phys.* **55**, 2061